A Liquid Crystal Model of Viral DNA Encapsidation

Shawn Walker
Department of Mathematics, Louisiana State University, Baton Rouge, LA, 70803

Javier Arsuaga*† and Mariel Vázquez*
Departments of Mathematics and Molecular and Cellular Biology†, University of California Davis, Davis, CA 95616*

Dmitry Golovaty
Department of Mathematics, University of Akron, Akron, OH 44325

M.Carme Calderer and Lindsey Hiltner
*School of Mathematics, University of Minnesota, Minneapolis, MN 55455**
(Dated: July 2, 2019)

A model of dsDNA packing for icosahedra bacteriophage viruses is developed and tested. The hexagonal chromonic structure of the dsDNA combined with its high resistance to bending are the main assumptions of the model. Furthermore, the modeling framework follows that of liquid crystals with variable degree of orientation, naturally allowing for the characterization of the disordered core region of the capsid, the decrease in pressure as the concentration of DNA in the capsid decreases during infection, as well as the location of possible defect structures in the DNA molecule. The model yields itself to the mathematical setting of finite element method, a main tool for prediction and design.

Double-stranded (ds)DNA bacteriophages are of renewed interest due to their use in medicine [1, 2] and biotechnology [1]. Icosahedral bacteriophages consist of a protein capsid with icosahedral symmetry whose assembly is followed by the packing, by a molecular motor, of a single naked dsDNA molecule [3]. The DNA molecule inside the viral capsid is found under extreme concentration and osmotic pressure. At the time of infection the DNA is released by a mechanism that suggests a phase transition, possibly into a 'liquid-like' state [4–6]. Both processes, packing and releasing of the genome, are highly dependent on how the DNA molecule folds inside the viral capsid; however our understanding of this folding remains very limited.

The concentration of the DNA molecule inside the viral capsid is between 200 and 800 mg/ml [7] and the estimated osmotic pressure ranges between 40 and 60 atmospheres [8, 9]. Three factors contribute to the excess pressure found inside the viral capsid: the decrease in entropy associated with the confinement imposed by the capsid, the high resistance of the DNA molecule to bending beyond its persistence length and the self-repulsion of the DNA molecule [10]. Experimental and theoretical studies acquired over the last 30 years [4, 11–16] have shown that under such conditions the DNA molecule forms a columnar hexagonal liquid crystal phase. In particular, liquid crystalline phases in bacteriophages were first proposed in [7], with an explicit reference to hexagonal packing made in [17] and since then, consistent data have been accumulating [13, 18–20].

A number of theoretical models, based on experimental and/or simulation data, have been proposed to describe the folding of the DNA molecule inside the bacteriophage capsid (e.g.[4, 12, 21–25]) with only few attempts to describe the DNA molecule in a liquid crystalline phase [20, 26]. These attempts however were based on energy fields originally proposed for modeling DNA molecules in free solution [13, 20, 24, 27–32] and do not provide adequate description of DNA inside the phage capsid.

In this article, we use cryo-electron microscopy (cryo-EM) data, the hexagonal chromonic liquid crystal structure of the packed DNA [17], and the continuum theory of liquid crystals to build a new model of DNA folding inside the viral capsid. The final packed structure of the DNA molecule corresponds to an energy minimizing configuration of the energy proposed below.

Our model assumes that the hydrated DNA fills the entire volume of the capsid [33] hence two relevant parameters are the molar c and volume c_v concentration of DNA. We take the customary point of view that the DNA molecule is a semiflexible elastic polymer characterized by the persistence length L_p which is about the size of the radius of the capsid. Since Cryo-EM data for most bacteriophages present multilayered spooling-like configurations on the outer layers of the packed genome [11, 21, 22, 34–37] we assume that the hexagonal chromonic structure provides a geometric scaffolding that sustains the trajectory of the DNA molecule. The decreasing available volume during DNA packing induces an extreme bending on the DNA molecule whose bending resistance prevents the hexagonal ordering from completely filling the capsid, so an inner core of disordered/isotropic DNA is assumed to form (See Figure 1) [34–37]. CryoEM data also suggest an axisymmetric cap-

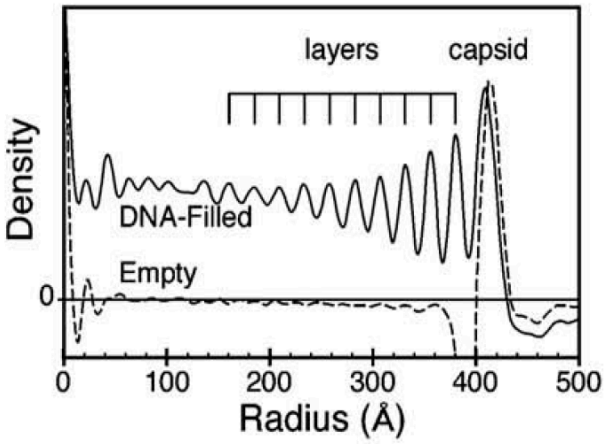

FIG. 1. DNA density of bacteriophage $T5$. The graph shows the radial density distribution of DNA inside the viral capsid. The dashed line shows the density of an empty capsid. Figure reproduced from [38]

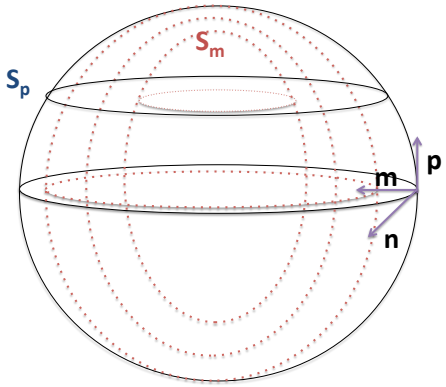

FIG. 2. This is a schematic representation of the level surfaces ω=constant, ϑ= constant, whose intersections provide the scaffolding that supports the DNA filament.

sid with parallel and meridian arrangements of the DNA molecule. Data at our disposal include: (1) cryoelectron images of the bacteriophage exhibiting capsid shape and protein core, the size and shape of the disordered region, the volume V of the capsid and the DNA density graphs that allow us to obtain the number, M, of concentric layers [34–37]; (2) ordering of the DNA molecule at the boundary as promoted by the capsid [12, 21, 22, 36]; (3) DNA effective diameter d and genome length L; (4) pressure measurements as well as speeds of DNA ejection [8, 11, 39–41].

To make our model precise, we assume that the capsid corresponds to a bounded, discretely axisymmetric region $\mathcal{B} \in \mathbb{R}^3$ with $\partial\mathcal{B}$ representing the piecewise smooth, faceted, viral capsid. We let $l_0 > 0$ denote the length of the axis that connects the location of the connector with its antipodal site in the viral capsid. Let $\Omega_0 \subset \mathcal{B}$ denote the isotropic region of the capsid, also taken to be axisymmetric with respect to l_0 and $\Omega := \mathcal{B} \setminus \Omega_0$, nonempty, denote the region occupied by the hexagonal chromonic liquid crystal phase. A piecewise smooth curve $\boldsymbol{r} = \boldsymbol{r}(s), s \in [0, L]$, describes the axis of the DNA. Note that, in general, the size of Ω_0 is an unknown of the problem.

The model of hexagonal chromonic liquid crystals that we present corresponds to that of de Gennes in the case of small distortions ([42], sec.7.1). A triple of linearly independent unit vectors $\boldsymbol{n}, \boldsymbol{m}, \boldsymbol{p}$ represents the uniaxial nematic director, along the direction tangent to the axis of the DNA molecule, and two local directions of ordering, respectively. The vectors $\boldsymbol{m}$ and $\boldsymbol{p}$ correspond to the lattice vectors of the columnar phase and account for the meridian and parallel arrangements. We will assume that the three vectors are almost mutually perpendicular in the sense made precise by the energy described below. In an energy minimizing configuration, these directions will be determined from their corresponding boundary values, that is, the filament organization in the contact with the capsid. Two complex valued functions $\psi = \rho e^{iq\omega}$ and $\gamma = \rho e^{iq\vartheta}$ account for the density of ordered material and describe the space filling conformation. Specifically, $\rho \geq 0$ gives the packing density of the layered molecules ($\rho = 0$ corresponds to disordered DNA) along the two preferred directions. The real number q corresponds to the frequency of the layers with $d = 2\pi/q$ representing the the effective diameter of the DNA and interlayer distance.

The chromonic structure is described by a discrete 2-family of level surfaces (see Figure 2)

$$\{\mathcal{S}^i_{\boldsymbol{m}}\}_{i=0}^{M} : \omega(\boldsymbol{x}) = id, \quad \{\mathcal{S}^j_{\boldsymbol{p}}\}_{j=0}^{P} : \vartheta(\boldsymbol{x}) = jd \qquad (1)$$

where M and $P = [\frac{l_0}{d}]$ (with brackets indicating the integer immediately below the value of the quotient) are nonzero positive integers. The first family corresponds to spheres concentric with the capsid while the second are the planes defined by z =constant. As part of satisfying the boundary conditions of the problem, we take $S^0_{\boldsymbol{m}} \equiv \partial\mathcal{B}$, with $j = 0$ corresponding to the parallel surface $z = -\frac{l_0}{2}$. These choices correspond to a spooling direction starting on the lower part of the capsid surface. The family of intersecting curves $\mathcal{C}_{i,j} = \mathcal{S}^i_{\mathbf{m}} \cap \mathcal{S}^j_{\mathbf{p}}$, $0 \leq i \leq M$, $0 \leq j \leq P$, give the location of the axis of the DNA molecule in the capsid and its ordering determines the direction of DNA spooling in the capsid. The final outcome, however, is independent of the ordering choices.

We propose that the total energy is given by the sum of the ordered chromonic phase plus the disordered isotropic core Ω_0 and a surface energy penalizing the interface be-

tween the two:

$$E = \int_\Omega F_{\text{Chr}}\, d\boldsymbol{x} + \nu \text{Vol}(\Omega_0) + \sigma \text{Area}(\partial\Omega_0), \text{ with} \quad (2)$$

$$F_{\text{Chr}} = F_{\text{N}}(\nabla \mathbf{n}, \mathbf{n}) + F_{\text{N}}(\nabla \mathbf{m}, \mathbf{m}) + F_{\text{N}}(\nabla \mathbf{p}, \mathbf{p}) + C_d\big(|\nabla\psi - iq\psi\mathbf{m}|^2 + |\nabla\gamma - iq\gamma\mathbf{p}|^2\big) + F_{\text{Rlx}}(\boldsymbol{n}, \boldsymbol{p}, \boldsymbol{m}) \quad (3)$$

$$F_{\text{N}}(\nabla \boldsymbol{n}, \boldsymbol{n}) = k_1(\nabla \cdot \boldsymbol{n})^2 + k_2(\boldsymbol{n} \cdot \nabla \times \boldsymbol{n})^2 + k_3|\boldsymbol{n} \times (\nabla \times \boldsymbol{n})|^2 + (k_2 + k_4)(\text{tr}\,(\nabla \boldsymbol{n})^2 - (\nabla \cdot \boldsymbol{n})^2) \quad (4)$$

$$F_{\text{Rlx}}(\boldsymbol{n}, \boldsymbol{m}, \boldsymbol{p}) = A(\mathbf{m} \cdot \mathbf{n})^2 + B(\mathbf{m} \cdot \mathbf{p})^2 + C(\mathbf{n} \cdot \mathbf{p})^2. \quad (5)$$

Not all the terms in the energy are relevant to the continuum theory. Assuming that k_1 and k_2 diverge near the phase transition to the hexagonal phase leads to a pure bending distortion at the limit ([42], sect 7.1; [43], page 315). The bending modulus is taken to be that of a semiflexible polymer in confinement, $k_3 = K_B T L_p I^{-1}$. I is the geometric moment of inertia with respect to the capsid axis. The value of I depends on the distance of the DNA molecule to to the capsid axis, and so, it accounts for the increase in bending resistance as the axis l_0 is approached. For simplicity, we associate the Oseen-Frank energy function $F_N(\nabla \boldsymbol{n}, \boldsymbol{n})$ to the director fields $\boldsymbol{m}$ and $\boldsymbol{p}$, expressing, in particular, high resistance to bending, to ensure a solid-like packing in the ordered region. This corresponds to the assumption that the filament properties also determine the geometry of packing. As for lyotropic liquid crystals, the energy density ν of the isotropic phase is assumed to be a function of the molar concentration c. Specifically, we use the approximate expressions derived by Onsager for lyotropic liquid crystals, that in large concentration regimes [44] take the form: $\nu = K_B T \ln(c^2 - \frac{45}{8} + c^{-2}) - 1$. The surface energy density $\sigma = K_B T \frac{0.257}{L_p d}$ is based on the Onsager's theory and derived in [45] for such regimes. (Approximations appropriate to low concentration regimes can also be found in the aforementioned references). The quantity C_d corresponds to the compressibility modulus. The volume concentration c_v, which measures how much of the capsid volume is occupied by DNA, together with the observation that the genome tends to fill the entire capsid [46] leads us to assume that $C_d = C_d(c_v)$ satisfying $C_d(0) = 0$, $C_d'(c_v) > 0$ and $\lim_{c \to 1^-} C_d(c_v) = +\infty$, the latter enforcing an idealized perfect packing structure at the limit of high concentrations. Note that these assumptions on C_d encode the phase transition solid to liquid-like behavior since the contribution of the chromonic phase will decrease as c_v decreases at the time of infection. The energy (5) allows for the relaxation of the orthogonality constraints between pairs of vectors $\boldsymbol{n}, \boldsymbol{m}, \boldsymbol{p}$. The positive constants A, B, C are then taken to be larger than the maximum dimensionless parameter of the energy. The combination of the energy terms (4) and (5) is analogous to the Ginzburg-Landau energy governing many condensed matter processes [47].

The role of the capsid proteins in promoting ordering of the DNA molecule dictates the choice of boundary conditions of the problem. If $\boldsymbol{m}_0$ denotes the normal vector to $\partial\mathcal{B}$ at a point $\boldsymbol{x} \in \mathcal{B}$ (where the normal is well defined) and $\boldsymbol{n}_0$ the unit tangent to the axis of the DNA at $\boldsymbol{x}$, we take $\boldsymbol{p}_0 := \boldsymbol{n}_0 \times \boldsymbol{m}_0$; note that $\boldsymbol{n}_0, \boldsymbol{m}_0$ and $\boldsymbol{p}_0$ form the local Frénet-Serret system associated with the curve through $\boldsymbol{x}$ and serve as Dirichlet boundary conditions for the unknown fields $\boldsymbol{n}, \boldsymbol{m}$ and $\boldsymbol{p}$. In addition, we require $\frac{\partial\omega}{\partial \boldsymbol{m}} = q$ and $\frac{\partial\vartheta}{\partial \boldsymbol{p}} = q$ at $\boldsymbol{x}$; this corresponds to an idealized perfect packing on the capsid surface.

In the case that the disordered core Ω_0 is a fixed region and the Frank constants, k_i, satisfy coercivity inequalities, standard methods of calculus of variations yield existence of a minimizer of the energy subject to the previously stated boundary conditions [48]. This configuration is piecewise smooth except for a discrete collection of singular points where $\boldsymbol{n} = 0$. These correspond to defects of the Oseen-Frank theory. Consequently, the level curves $\mathcal{C}_{ij}$ are piecewise smooth.

The reconstitution of the trajectory of the dsDNA molecule is achieved by subsequently solving the initial value problem for the ordinary differential equation $\boldsymbol{r}'(s) = \boldsymbol{n}(\boldsymbol{r}(s))$, $|\boldsymbol{n}| = 1$, $s \in [0, l]$ with $r(\mathbf{0}) = \boldsymbol{r}_0$, where $\boldsymbol{r}_0$ represents the location of the attached filament tip at the entrance of the capsid. The solution curve $\boldsymbol{r}(s)$ describing the trajectory of the DNA axis is piecewise differentiable and provides the parametrization of the curves $\mathcal{C}_{i,j}$; it becomes singular at the liquid crystal defect locations $\boldsymbol{n} = \mathbf{0}$. The latter are also the sites where the filament transitions from the curve segment $\mathcal{C}_{i,j}$ to either $\mathcal{C}_{i,j+1}$ or $\mathcal{C}_{i+1,j}$, following the direction of spooling.

Filament crossings within a curve segment $\mathcal{C}_{i,j}$ also correspond to liquid crystal defects. These include: (a) dislocations, points with $\rho = 0$, where two or more layers of the same family come into contact allowing the filament to break the order of transition from $\mathcal{C}_{i,j}$ to $\mathcal{C}_{i+1,j}$; (b) point defects where the curve becomes singular and filament contacts may take place to perform a crossing;

Virus	L_p	d	c	L (nm)	R (nm)	r_0/R
T4	1.32	0.06	21.37	55047.6	40.0	0.5500
T5	1.39	0.07	17.85	39423.8	42.0	0.4286
T7	2.03	0.10	18.17	12932.0	26.05	0.5889
ϵ15	1.9	0.09	13.98	12846.0	28.37	0.5735

TABLE I. Physical measurements of four different bacteriophages.The symbol L_P denotes the persistence length of a DNA chain of length L, effective diameter d, molar concentration c in a sphere-like capsid of radius R with a measured radius r_0 of the disordered core. T4 [50, 51]; T5 [36]; T7 [21]; ϵ15 [37].

(c) point defects of order $\pm\frac{1}{2}$ where the filament loses orientation [49]. With the model in hand we address two key questions about the bacteriophage structure: (1)the osmotic pressure, and (2) the size of the isotropic region. The calculation of the Cauchy stress tensor $\mathbb{T}$ associated with the total energy (2) follows a standard variational approach, formally expressed as $\mathbb{T} = \delta E/\delta \mathbf{x}$ are standard. The pressure near the surface of the capsid is then given by $P = \boldsymbol{\nu}^T \mathbb{T} \boldsymbol{\nu}$, with $\boldsymbol{\nu}$ denoting the unit outer normal to the surface that on each tested conformation (TABLE I) has the form

$$P(r) = \frac{L_p}{\pi r^5} \cdot \frac{R_g T \rho_{\text{DNA}}}{M_{\text{DNA}}} \quad \text{with } r = 1,$$

where R_g is the universal gas constant; $T = 310$K is the temperature; $\rho_{\text{DNA}} = 1.7\frac{\text{g}}{\text{cm}^3}$ is the density of (ds)DNA, and $M_{\text{DNA}} = 650\frac{\text{g}}{\text{mol}}$ its molar mass. (The ejection force at each point corresponds to the tangential component of $\mathbb{T}\boldsymbol{\nu}$). The fifth column in Table II shows the predicted pressures. They fall within the range of the experimentally measured forces on the capsid [8, 41], with bacteriophages $T4$ and $T5$ having smaller values.

Next we estimated the size of the disordered (isotropic) core. In this study we assume that the capsid has the shape of a sphere equally truncated at the poles, with DNA spooled around its distinguished axis, with cylindrically arranged layering. We prescribe the vector fields according to the geometry, so that $\boldsymbol{n} = \boldsymbol{e}_\theta, \boldsymbol{m} = -\boldsymbol{e}_r$ and $\boldsymbol{p} = \boldsymbol{e}_z$, with layer locations given by the level surfaces of ω and γ (1), and such that $\boldsymbol{m} = q\nabla\omega$ and $\boldsymbol{p} = q\nabla\theta$. Substituting these fields into (3), we minimize the resulting energy (2) with respect to the unknown isotropic core radius r_0. TABLE II shows the the data used in these calculations (column 2), the predicted value (column 3) and the estimated error(column 4). Our proposed model can be easily extended to incorporate other assumptions and data. First, the model is purely geometrical and mechanical, although it implicitly and partially accounts for electrostatic repulsion and ionic effects, since it incorporates the value of the effective diameter of the DNA under confinement. Although Tables I and II show fairly accurate predictions of the isotropic core size for the probed viruses, the lower values obtained for the corresponding pressure seem to indicate the need to explicitly include ionic and electrostatic effects. A model explicitly accounting for these effects, including those of an ionic environment by assigning permeability to the capsid, is currently being developed by the authors. Second, it follows as a consequence of the unit director length constraint that the curve $\mathbf{r}(s)$ must satisfy $|\mathbf{r}'(s)| = 1$, so the DNA filament is inextensible. However, there is evidence that under certain conditions, DNA may stretch to the point of breaking down its double helix structure (reviewed in [52]). In future work, the constraint of unit director length will be relaxed by including the penalty term $(|\mathbf{n}(\mathbf{x})|^2 - 1)^2$. Third, the model also allows for departure from the deterministic packing by the incorporation of appropriate random noise terms which will help explain the formation of knots in some bacteriophages [28, 29]. Fourth, the description of the capsid domain can also be modified to cases when the protein complex that includes the molecular motor protrudes inside the volume determined by the capsid. Although it does not pose any significant mathematical complications, it does provide a mechanism to resolve the polar defects that would, otherwise, be present in such a geometric liquid crystal configuration. Fifth, our model is also amenable to be combined with parameter determining optimization methods, making it appropriate to broader designing features required in applications in medicine and biotechnology. Sixth, chiral configurations can also be treated extending the current model to include chiral effects in the energy and taking into account the imprinted protein twist configurations on the boundary of the capsid. Finally, the present model neglects thermal effects that may be relevant to certain type of viruses (e.g. the human Herpes HSV-1) that will be addressed in future works.

Virus	Measured Core Size	Predicted Core Size	Error	P(atm)
T4	0.5500	0.5100		28.70
T5	0.4286	0.3968		30.17
T7	0.5889	0.5212		44.02
ϵ15	0.491235	0.569		40.41

TABLE II. Predicted size of the disordered phase and osmotic pressure for different bacteriophages. The table lists the measured and predicted radii of the isotropic for several viruses. The values are scaled by the corresponding capsid radii as listed in Table I, The percentage error is the difference between the measured and predicted size of the isotropic phase, divided by the measured core size. In the calculation for T5 and ϵ15, the expressions of the material parameters ν [44] and σ [53] correspond to the approximation in the low concentration regime. The evaluations for the other entries in the table are taken at the high concentration limits [54–56]. The last column lists the pressure calculated near the capsid boundary.

* *Arsuaga and Vázquez gratefully acknowledge support from the grant DMS/NIGMS R01 GM109457. Vázquez also knowledges the support from the CAREER grant DMS1057284 and DMS1716987.* Calderer is very grateful for the support provided by grants DMS-DMREF 1435372 and DMS-1542200.

[1] I. U. Haq, W. N. Chaudhry, M. N. Akhtar, S. Andleeb, and I. Qadri, Virology journal **9**, 9 (2012).
[2] A. Sulakvelidze, Z. Alavidze, and J. G. Morris, Antimicrobial agents and chemotherapy **45**, 649 (2001).
[3] D. E. Smith, S. J. Tans, S. B. Smith, S. Grimes, D. L. Anderson, and C. Bustamante, Nature **413**, 748 (2001).
[4] A. Leforestier and F. Livolant, Journal of molecular biology **396**, 384 (2010).
[5] T. Liu, U. Sae-Ueng, D. Li, G. C. Lander, X. Zuo, B. Jönsson, D. Rau, I. Shefer, and A. Evilevitch, Proceedings of the National Academy of Sciences **111**, 14675 (2014).
[6] U. Sae-Ueng, D. Li, X. Zuo, J. B. Huffman, F. L. Homa, D. Rau, and A. Evilevitch, Nature chemical biology **10**, 861 (2014).
[7] E. Kellenberger, E. Carlemalm, J. Sechaud, A. Ryter, and G. De Haller, in *Bacterial chromatin* (Springer, 1986) pp. 11–25.
[8] A. Evilevitch, L. Lavelle, C. M. Knobler, E. Raspaud, and W. M. Gelbart, Proceedings of the National Academy of Sciences **100**, 9292 (2003).
[9] M. Jeembaeva, M. Castelnovo, F. Larsson, and A. Evilevitch, Journal of molecular biology **381**, 310 (2008).
[10] S. C. Riemer and V. A. Bloomfield, Biopolymers **17**, 785 (1978).
[11] A. Leforestier and F. Livolant, Proceedings of the National Academy of Sciences **106**, 9157 (2009).
[12] J. Lepault, J. Dubochet, W. Baschong, and E. Kellenberger, The EMBO journal **6**, 1507 (1987).
[13] D. Reith, P. Cifra, A. Stasiak, and P. Virnau, Nucleic acids research **40**, 5129 (2012).
[14] R. L. Rill, Proceedings of the National Academy of Sciences **83**, 342 (1986).
[15] T. E. Strzelecka, M. W. Davidson, and R. L. Rill, Nature **331**, 457 (1988).
[16] H.-S. Park, S.-W. Kang, L. Tortora, Y. Nastishin, D. Finotello, S. Kumar, and O. D. Lavrentovich, The Journal of Physical Chemistry B **112**, 16307 (2008).
[17] F. Livolant, Physica A: Statistical Mechanics and its Applications **176**, 117 (1991).
[18] A. Leforestier and F. Livolant, Biophysical journal **65**, 56 (1993).
[19] A. Leforestier, S. Brasiles, M. De Frutos, E. Raspaud, L. Letellier, P. Tavares, and F. Livolant, Journal of molecular biology **384**, 730 (2008).
[20] D. Marenduzzo, E. Orlandini, A. Stasiak, L. Tubiana, C. Micheletti, *et al.*, Proceedings of the National Academy of Sciences **106**, 22269 (2009).
[21] M. E. Cerritelli, N. Cheng, A. H. Rosenberg, C. E. McPherson, F. P. Booy, and A. C. Steven, Cell **91**, 271 (1997).
[22] W. C. Earnshaw and S. R. Casjens, Cell **21**, 319 (1980).
[23] N. V. Hud, Biophysical journal **69**, 1355 (1995).
[24] A. S. Petrov, M. B. Boz, and S. C. Harvey, Journal of structural biology **160**, 241 (2007).
[25] P. Serwer, S. J. Hayes, and R. H. Watson, Journal of molecular biology **223**, 999 (1992).
[26] J. Arsuaga and Y. Diao, Computational and Mathematical Methods in Medicine **9**, 303 (2008).
[27] J. Arsuaga, R. K.-Z. Tan, M. Vazquez, S. C. Harvey, *et al.*, Biophysical chemistry **101**, 475 (2002).
[28] J. Arsuaga, M. Vázquez, S. Trigueros, J. Roca, *et al.*, Proceedings of the National Academy of Sciences **99**, 5373 (2002).
[29] J. Arsuaga, M. Vazquez, P. McGuirk, S. Trigueros, J. Roca, *et al.*, Proceedings of the National Academy of Sciences of the United States of America **102**, 9165 (2005).
[30] D. Marenduzzo, C. Micheletti, E. Orlandini, *et al.*, Proceedings of the National Academy of Sciences **110**, 20081 (2013).
[31] G. C. Rollins, A. S. Petrov, and S. C. Harvey, Biophysical journal **94**, L38 (2008).
[32] A. J. Spakowitz and Z.-G. Wang, Biophysical journal **88**, 3912 (2005).
[33] E. Kellenberger, E. Carlemalm, J. Sechaud, A. Ryter, and G. De Haller, Bacterial chromatin **1**, 11 (1986).
[34] L. R. Comolli, A. J. Spakowitz, C. E. Siegerist, P. J. Jardine, S. Grimes, D. L. Anderson, C. Bustamante, and K. H. Downing, Virology **371**, 267 (2008).
[35] J. Chang, P. Weigele, J. King, W. Chiu, and W. Jiang, Structure **14**, 1073 (2006).
[36] G. Effantin, P. Boulanger, E. Neumann, L. Letellier, and J. Conway, Journal of molecular biology **361**, 993 (2006).
[37] W. Jiang, J. Chang, J. Jakana, P. Weigele, J. King, and W. Chiu, Nature **439**, 612 (2006).
[38] I. J. Molineux and D. Panja, Nature reviews. Microbiology **11**, 194 (2013).
[39] A. Cordova, M. Deserno, W. M. Gelbart, and A. Ben-Shaul, Biophysical journal **85**, 70 (2003).
[40] P. Grayson, A. Evilevitch, M. M. Inamdar, P. K. Purohit, W. M. Gelbart, C. M. Knobler, and R. Phillips, Virology **348**, 430 (2006).
[41] S. Tzlil, J. T. Kindt, W. M. Gelbart, and A. Ben-Shaul, Biophysical journal **84**, 1616 (2003).
[42] P. G. de Gennes and J. Prost, *The physics of liquid crystals* (Oxford University Press, 1993).
[43] M. Kleman and O. D. Laverntovich, *Soft matter physics: an introduction* (Springer Science & Business Media, 2007).
[44] L. Onsager, Annals of the New York Academy of Sciences **51**, 627 (1949).
[45] M. Doi and N. Kuzuu, J. Appl. Polym Sci: Appl. Polym. Symp. **41**, 65 (1985).
[46] P. K. Purohit, M. M. Inamdar, P. D. Grayson, T. M. Squires, J. Kondev, and R. Phillips, Biophysical journal **88**, 851 (2005).
[47] V. Ginzburg and L. Landau, Zh. Eksp. Teor. Fiz. **20**, 164 (1950).
[48] R. Hardt, D. Kinderlehrer, and F. H. Lin, Comm. Math. Phys. **105**, 547 (1987).
[49] J. M. Ball and A. Zarnescu, Molecular Crystals and Liquid Crystals **495**, 221 (2008).
[50] P. Leiman, S. Kanamaru, V. Mesyanzhinov, F. Arisaka, and M. Rossmann, Cellular and Molecular Life Sciences **60**, 2356 (2003).
[51] N. H. Olson, M. Gingery, F. A. Eiserling, and T. S. Baker, Virology **279**, 385 (2001).
[52] C. Bustamante, Z. Bryant, and S. B. Smith, Nature **421**,

423 (2003).
[53] N. Kuzuu and M. Doi, J. Phys. Soc. Japan **53**, 1031 (1984).
[54] S. Wolfsheimer, C. Tanase, K. Shundyak, R. Van Roij, and T. Schilling, Physical Review E **73**, 061703 (2006).
[55] R. van Roij, European journal of physics **26**, S57 (2005).
[56] N. Priezjev and R. A. Pelcovits, Physical Review E **62**, 6734 (2000).